mol % naphthyl-containing segments. A major difference between poly(1-vinylnaphthalene) and its copolymers would, of course, be in the nature of the end groups and in the type of chain coiling since the copolymer chains are undoubtedly longer than the homopolymer chains. If the event of phosphorescence occurs at the chain ends in a delocalizing system such as this, then the shift may be accounted for, but at present such explanations are not satisfactory.

As long as coupling can occur between aromatic rings along a polymer chain, it would appear that intramolecular energy transfer is possible. Triplet energy transfer has been demonstrated here; singlet transfer has not been excluded. Since energy can be transferred from one type of copolymer segment to another and, at least in the present instances, the accepting segment can eliminate the energy radiatively, it may be possible to photostabilize certain polymers by incorporating energy acceptors into the chain. A knowledge of energy levels is necessary; the lowest triplet energy levels for alkylbenzenes and 1-alkylnaphthalenes are about 29 and 21 kK, respectively, and the transfer of energy is in the direction predicted by these values. In effect, polystyrene should be stabilized in regard to absorbed energy by the substitution of a small number of naphthyl groups for phenyl groups along the chain.

Conclusions

Intramolecular triplet energy transfer has been shown to take place in polystyrene in a rigid matrix. In copolymers of styrene and 1-vinylnaphthalene, intramolecular triplet energy transfer occurs from styrene-derived segments to 1-vinylnaphthalene-derived segments. A radiatively emitting copolymer segment or, by implication, homopolymer end group can be utilized as the detector of intramolecular energy transfer. Intramolecular energy transfer can be utilized in certain cases to obtain direct evidence of copolymer chain sequence distribution.

Structure of Poly(ethylene oxide) Complexes. III. Poly(ethylene oxide)–Mercuric Chloride Complex. Type II

Masaaki Yokoyama, Hideaki Ishihara,[1a] Reikichi Iwamoto,[1b] and Hiroyuki Tadokoro[1c]

Department of Polymer Science, Faculty of Science, Osaka University, Toyonaka, Osaka, Japan. *Received December 20, 1968*

ABSTRACT: The structure of the crystalline complex of poly(ethylene oxide)–mercuric chloride type II has been determined by X-ray diffraction and infrared absorption methods. The unit cell is orthorhombic with the lattice constants, a = 7.75 Å, b = 12.09 Å, c (fiber axis) = 5.88 Å, and the unit cell contains four $HgCl_2$ molecules and four CH_2CH_2O units. Two poly(ethylene oxide) chains pass through the lattice. The space group consistent with the systematic absences is Pncm-D_{2h}[7] or Pnc2-C_{2v}[6]. The positions of the Hg and Cl atoms can be determined by X-ray diffraction method. The molecular structure of poly(ethylene oxide) has been deduced by means of far-infrared absorption and normal coordinate treatments. The conformation of poly(ethylene oxide) in the complex of type II has been found to be the form near to $TG_2T\bar{G}_2$; that is

$$-CH_2-(-\underset{167^\circ}{O}-\underset{81^\circ}{CH_2}-\underset{73^\circ}{CH_2}-\underset{-167^\circ}{O}-\underset{-81^\circ}{CH_2}-\underset{-73^\circ}{CH_2}-)_n-$$

This molecular structure has been confirmed by the improvement of the agreement between the observed and calculated structure factors, and by the reasonable entry of this model into the interstice of the unit cell between $HgCl_2$ molecules.

In a previous paper[2a] it has been reported that poly(ethylene oxide) (PEO)[2b,3] forms two kinds of crystalline complexes with mercuric chloride, one of which consists of mole ratio of $4CH_2CH_2O:1HgCl_2$ and the other consists of mole ratio of $1CH_2CH_2O:1HgCl_2$. The structure of the former crystalline complex, denoted as type I, was determined by X-ray analysis, and the conformation of PEO in type I was found to be the $T_5GT_5\bar{G}$ form.

In the present work we have studied the crystal structure of the latter crystalline complex, denoted as type II, by use of X-ray diffraction and infrared absorption methods. On the analysis of type II, it is very difficult to determine the molecular structure of PEO by X-ray diffraction alone, because the contribution of heavy atoms (Hg, atomic number 80; Cl, 17) to the structure factors in type II is much larger than that in type I. In such a case the far-infrared absorption method is very useful, where some bands are strongly sensitive to the molecular conformation of PEO. The molecular conformation of PEO can be deduced by comparison of the observed data with the calculated frequencies by the normal coordinate treatment for a suitable model. The PEO model thus obtained will be confirmed by the reasonable entry into the interstice of the unit cell between $HgCl_2$ molecules. It seems

(1) (a) Katata Research Institute, Toyobo Co., Ltd., Honkatata, Otsu City, Shiga, Japan. (b) Government Industrial Research Institute, Osaka, Midorigaoka, Ikeda City, Osaka, Japan. (c) To whom correspondence should be addressed.

(2) (a) R. Iwamoto, Y. Saito, H. Ishihara, and H. Tadokoro, *J. Polym. Sci., Part A-2*, **6**, 1509 (1968); (b) H. Tadokoro, T. Yoshihara, Y. Chatani, S. Tahara, and S. Murahashi, *Makromol. Chem.*, **73**, 109 (1964).

(3) T. Miyazawa, *J. Chem. Phys.*, **35**, 693 (1961).

TABLE I

OBSERVED FREQUENCIES OF PEO–MERCURIC HALIDE COMPLEXES (TYPE II) IN THE FAR-INFRARED REGION

PEO–$HgCl_2$ ν_{obsd}, cm^{-1}	PEO–$HgBr_2$[a] ν_{obsd}, cm^{-1}	Descriptions
567 (∥, ⊥) m		
505 (⊥) m		
443 (⊥) m	439 m	
378 (∥, ⊥) s	372 s	
345 (...) vvs		$HgCl_2$ antisymmetric stretching
280 (⊥) m		
255 (⊥) w (sh)	250 w (sh)	
245 (∥, ⊥) m		
	245 vvs	$HgBr_2$ antisymmetric stretching + PEO
211 (⊥) m	210 w	
158 (∥, ⊥) m	153 m	
94 (...) vvs		$HgCl_2$ bending

[a] Measured on the Nujol mull.

very interesting to elucidate what kind of conformation of the polymer chain in the complex can be stable.

Experimental Section

Since the preparation of the complex was described in a previous paper,[2a] further description about the sample will not be given in this paper.

I. X-Ray Diffraction. The X-ray photographs were taken by using Ni-filtered Cu $K\alpha$ radiation. All observed reflections in the X-ray fiber pattern could be indexed with the orthorhombic unit cell: a = 7.75 Å, b = 12.09 Å, c (fiber axis) = 5.88 Å. The density measurement was made by flotation method, and the density of type II was found higher than 3.31 g/cc, since the sample sinks quickly in diiodomethane (CH_2I_2, 3.31 g/cc). Then the observed value (>3.31 g/cc) was consistent with the calculated one (3.79 g/cc) by assuming that four $HgCl_2$ molecules and four CH_2CH_2O units of PEO are contained in the unit cell. The lattice constants were refined by the measurement on the powder sample with a diffractometer calibrated with NaCl.

The systematic absences were observed in the fiber diagram as $0kl$, $k + l \neq 2n$; and $h0l$, $l \neq 2n$. The space groups consistent with the systematic absences are Pncm-D_{2h}^7 and Pnc2-C_{2v}^8. The integrated intensities were measured on the powder sample by a diffractometer up to the angle 2θ = 70°. The number of the observed reflections was 67. The intensity data measured on the fiber diagrams by a multiple pack method were used for the separation of the overlapped reflections measured on the powder sample after the Lorentz polarization correction. Furthermore, the overlapped reflections which could not be separated even on the fiber diagram were estimated as proportional to the calculated intensities.

II. Infrared Absorption Spectrum. The infrared absorption spectra of the complex type II in the region from 4000 to 500 cm^{-1} were measured by a Japan Spectroscopic Co. DS-402G grating infrared spectrophotometer. The polarization measurements were made with AgCl polarizers. Far-infrared spectra in the region from 500 to 80 cm^{-1} were recorded by a Hitachi Model FIS-1 double beam far-infrared spectrophotometer with a transmission polarizer of polyethylene sheets. The polarized far-infrared spectra of the PEO–$HgCl_2$ complex of type II are shown in Figure 1, together with that of $HgBr_2$ complex of type II. Since the crystal structure of $HgBr_2$ complex of type II was found to be isomorphous to that of the $HgCl_2$ complex of type II by X-ray diffraction as reported in the previous paper,[2a] the far-infrared absorption bands due to the PEO molecule were identified by the comparison between those two spectra as

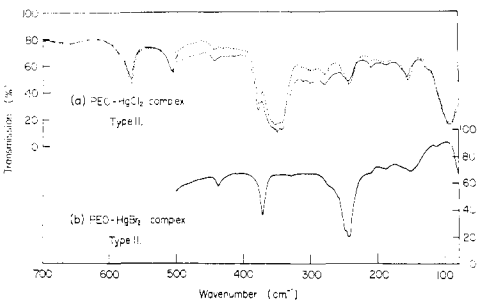

Figure 1. (a) Far-infrared spectra of PEO–$HgCl_2$ complex (700–80-cm^{-1} region). The solid (or broken) curves give the spectra measured by the polarized radiation with the electric vector perpendicular (or parallel) to the fiber axis (b) Far-infrared spectrum of PEO–$HgBr_2$ complex measured by the Nujol mull method.

shown in Table I. Since we could not prepare so highly oriented sample of the pure type II as type I, the dichroisms of some bands were determined from the bands of type II observed on the highly oriented films, which are on the way of the transition from type I to type II.

Determination of The Structure

I. Position of the $HgCl_2$ Molecules in the Unit Cell. The three-dimensional Patterson function was calculated by using the intensity data measured on the powder sample. The analysis was carried out by assuming Pncm-D_{2h}^7 for simplicity. The Patterson functions $P(u, v, 0)$ and $P(u, v, 1/2)$ were interpreted reasonably in terms of the interatomic vectors of Hg···Hg and Hg···Cl, by assuming that the four Hg atoms lie in the fourfold special positions on the mirror plane and that two Cl atoms bonded to a Hg atom are on the same mirror plane. These two Cl atoms are not crystallographically equivalent to each other.

The structure factors calculated on the basis of the positions of the Hg and Cl atoms obtained from the Patterson function resulted in a fairly good agreement with the observed structure factors. The atomic parameters of Hg and Cl were refined by repetition of Fourier syntheses so as to improve the agreement between the observed and calculated structure factors.

It is very difficult to obtain the electron density distribution of the PEO molecule by the Fourier synthesis,

TABLE II

FACTOR GROUP ANALYSIS FOR THE SKELETAL MODEL AND SELECTION RULE

C_s	E	σ_g	N_i[a]	Ir
A′	1	1	$9 - 2(T_x, T_z)$	A(∥, ⊥)
A″	1	−1	$9 - 2(T_y, R_x)$	A(⊥)

[a] N_i, the number of normal modes. T, R, translation and rotation of a molecule as a whole.

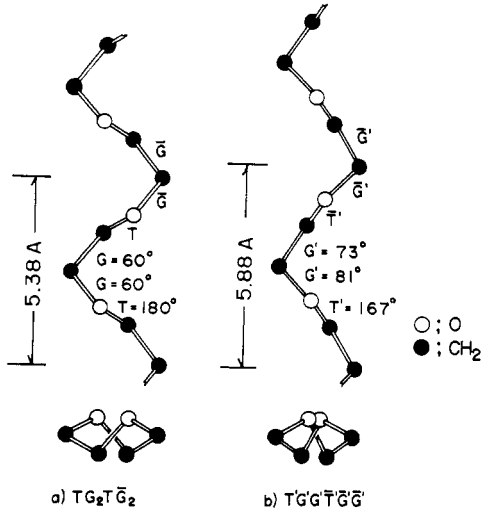

Figure 2. Molecular model of PEO in the complex of type II: (a) starting model, $TG_2T\bar{G}_2$; and (b) most plausible model, $T'G'_2\bar{T}'\bar{G}'_2$.

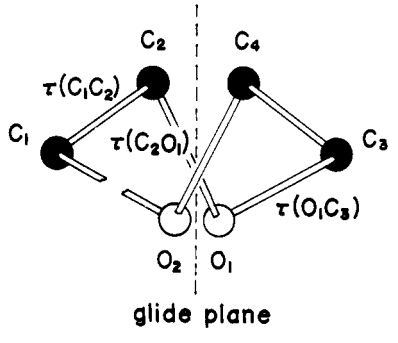

Figure 3. Numbering of the atoms.

because, as already mentioned, the contribution of heavy atoms to the structure factors in type II is much larger than that in type I. It can be seen how large their contribution is, by comparing the contribution of heavy atoms with that of PEO at Bragg angle $\theta = 0°$; for type I

$$f_{Hg}^2 + 2f_{Cl}^2\ (=6978) \gg 4(2f_c^2 + f_o^2)\ (=544)$$

for type II

$$f_{Hg}^2 + 2f_{Cl}^2\ (=6978) \gg 2f_c^2 + f_o^2\ (=136)$$

The determination of the molecular structure was made by studying the infrared absorption bands in the far-infrared region, where some bands are strongly sensitive to the conformation of the molecule.

II. Conformation of PEO in the Complex. a. A Molecular Model. From the X-ray diffraction the fiber period of type II was found to be 5.88 Å. This value is a half of the fiber period (11.75 Å) of type I. This may suggest that two monomeric units (CH_2CH_2O) constitute the fiber period, since the fiber period of type I consists of four monomeric units. Furthermore, since it is presumed that the spatial arrangement of the O atoms of PEO and the Hg atoms are similar as in the case of type I, where the C–C bond in the OCH_2CH_2O part coordinating to a Hg atom takes the *gauche* form, the internal rotation angle about the C–C bond in type II may take also a *gauche* form. Accordingly, we examined the molecular model with *gauche* conformation of the C–C bond. As a result, the reasonable molecular model having the $TG_2T\bar{G}_2$ conformation was obtained, which gives the calculated fiber period 5.38 Å. Here G and $\bar{G}$ mean the right- and

$$-CH_2-(-O-CH_2-CH_2-O-CH_2-CH_2-)_n$$
$$\quad T \quad G \quad G \quad T \quad \bar{G} \quad \bar{G}$$

left-handed *gauche* forms, respectively. In Figure 2a is shown this model, which has only a glide symmetry along the fiber axis, and its symmetry is, therefore, isomorphous to the point group C_s.

First of all, it was examined whether the model is suitable, by comparing the number of the observed bands with the result of the factor group analysis. In Table II are given the number of the normal frequencies and the selection rules under the factor group C_s. From the selection rules, it can be expected that four bands of the A′ species (parallel or perpendicular) and four bands of the A″ species (perpendicular) are observed in the far-infrared region from 700 to 80 cm^{-1}. Here the C–O and C–C stretching modes are not taken into account, since these stretching bands may be observed in the region higher than 700 cm^{-1}. The number of the bands to be expected from the factor group analysis are consistent with the observed data shown in Table I. The model, however, possesses a difficulty that the *gauche* conformation about the C–O bond seems to be not suitable from the view point of interatomic distances[4] between nonbonded hydrogen atoms. The nearest H···H distance for the $TG_2T\bar{G}_2$ model was found to be 1.73 Å by assuming the bond length (C–H = 1.09 Å) and the tetrahedral bond angles. The interatomic distance 1.73 Å is much shorter than the sum of the van der Waals radii of hydrogen atoms 2.2 Å.[5] It is, however, believed from the results of the factor group analysis that this $TG_2T\bar{G}_2$ model is not far from the true structure of PEO, and this is suggested from the normal coordinate treatment for the skeletal vibrations as described in the following step.

The skeletal normal vibrations were calculated for the far-infrared region according to the Wilson's GF-matrix method.[6] Here the methylene group was considered as a united atom with the atomic weight of CH_2. In the calculation the Urey–Bradley force field[7] was used, which was the same set of the force constants used in the case of determining the normal helical structure

(4) J. E. Mark and P. J. Flory, *J. Amer. Chem. Soc.*, **87**, 1415 (1965).
(5) L. Pauling, "The Nature of the Chemical Bond," 3rd ed, Cornell University Press, Ithaca, N. Y., 1960.
(6) E. B. Wilson, Jr., J. C. Decius, and P. C. Cross, "Molecular Vibrations," McGraw-Hill Book Co., Inc., New York, N. Y., 1955.
(7) H. G. Urey and C. A. Bradley, *Phys. Rev.*, **38**, 1969 (1931).

TABLE III

FORCE CONSTANTS[a]

	$TG_2T\bar{G}_2$, mdyn/Å	$T'G'_2\bar{T}'\bar{G}'_2$, mdyn/Å
K(CO)	4.38	4.35
K(CC)	3.70	3.95
H(COC)	0.20	0.34
H(CCO)	0.20	0.25
F_τ(CC)	0.0495	0.0605
F_τ(CO)	0.0456	0.0613
F(CC)	0.30	0.41
F(CO)	0.60	0.39
F'	$-0.1F$	$-0.1F$

[a] The force constants, K, H, F_τ, and F indicate the stretching, bending, torsional, and repulsive force constants, respectively.

of PEO,[2b] as shown in column 2 of Table III. The numerical computations were carried out by using the NEAC-2200 Model 500 electronic digital computer (Nippon Electric Co., Ltd.) installed in the Computation Center of this university. The calculated frequencies are listed in Table IV, together with the observed data. From the table it is obvious that the calculated frequencies are in fairly good agreement with the observed ones.

b. Refinement of the Molecular Model. Although we could confirm the molecular model to be fairly well, the too-short distance between nonbonded hydrogen atoms, as mentioned, remained unsettled. Furthermore, the calculated fiber period 5.38 Å is a little shorter than the observed one (5.88 Å). Accordingly, we tried to change the internal rotation angles so as to satisfy the following conditions: (a) the molecular model must be retained under the glide symmetry C_{2v}, (b) the calculated fiber period is equal to the observed one, and finally (c) the hydrogen atom must be farthest from each other.

First, we examined such relation between the internal rotation angles (*i.e.*, $\tau(C_1C_2)$, $\tau(C_2O_1)$, and $\tau(O_1C_3)$, as shown in Figure 3) that may satisfy conditions a and b. The mathematical procedure reported by Ganis and Temussi[8] was applied in order to correlate the conformational parameters of the structural unit with the geometrical parameters of a polymer chain.

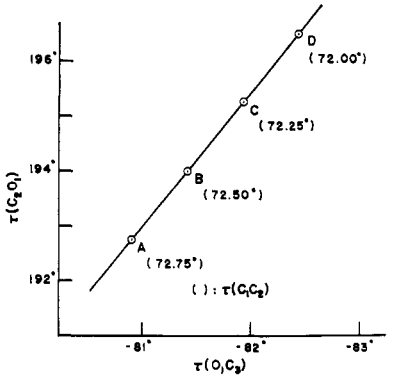

Figure 4. Relationship between internal rotation angles that satisfy the molecular symmetry and the fiber period.

The direction perpendicular to the glide plane is defined as a vector **V**

$$\mathbf{V} = [\mathbf{H}(C_1C_3) \times \mathbf{H}(C_2C_4)] \times [\mathbf{H}(C_4C_3) + \mathbf{H}(C_2C_1)]$$

where $\mathbf{H}(i, j)$ denotes the vector joining the ith atom with the jth atom, and the subscripts denote the atoms shown in Figure 3.

If the glide symmetry is retained, relations 1 and 2 must be satisfied.

$$[\mathbf{H}(C_1C_3) \times \mathbf{H}(C_2C_4)] \cdot \mathbf{H}(O_1O_2) = 0 \quad (1)$$

$$[\mathbf{H}(O_1C_2) + \mathbf{H}(O_2C_4)] \cdot \mathbf{V} = 0 \quad (2)$$

On the assumption that the bond length C–O = 1.43 Å, C–C = 1.54 Å, and the bond angles OCC = COC = 109° 28′ (tetrahedral angle) we calculated each vector, $\mathbf{H}(i, j)$, in terms of the cartesian coordinates of the atoms, and examined the above conditions among the vectors. As a result, these internal rotation angles, $\tau(C_1C_2)$, $\tau(C_2O_1)$, and $\tau(O_1C_3)$, which satisfy the conditions given in eq 1 and 2, and in b, are connected with each other by the relationship shown in Figure 4. In the figure the abscissa and the ordinate

(8) P. Ganis and P. A. Temussi, *Makromol. Chem.*, **89**, 1 (1965).

TABLE IV

SKELETAL VIBRATIONS OF PEO–$HgCl_2$ COMPLEX TYPE II

Species	Obsd frequencies, cm^{-1}	Calcd frequencies,[a] cm^{-1} $TG_2T\bar{G}_2$	Calcd frequencies,[a] cm^{-1} $T'G'_2\bar{T}'\bar{G}'_2$	Assignment (PED %)[b]
	1100 (∥, ⊥) s	1057	1097	ν(CC)(58) − ν_s(CO)(33)
		955	1093	ν_a(CO)(88)
	923 (∥, ⊥) s	921	931	ν_s(CO)(51) + ν(CC)(24) + δ(COC)(12)
A′	567 (∥, ⊥) m	573	557	δ_a(CCO)(80)
	378 (∥, ⊥) s	408	443	δ(COC)(54) − δ_s(CCO)(17)
	245 (∥, ⊥) m	253	269	δ_s(CCO)(40) − τ(CC)(25) − δ(COC)(19)
	158 (∥, ⊥) m	143	142	τ_a(CO)(74) + τ_s(CO)(18)
	1154 (⊥) m	1053	1146	ν_a(CO)(60) − ν(CC)(37)
	1046 (⊥) s	982	1009	ν_s(CO)(77)
	1015 (⊥) s	927	981	ν(CC)(55) + ν_a(CO)(30)
A″	505 (⊥) m	480	520	δ(COC)(45) + δ_a(CCO)(25)
	443 (⊥) m	462	462	δ_a(CCO)(65) − δ_a(CCO)(20)
	255 (⊥) sh	233	256	δ_a(CCO)(32) + τ(CC)(26) + τ_a(CO)(14)
	211 (⊥) m	192	204	δ(COC)(37) − τ_s(CO)(28) + τ_a(CO)(11)

[a] The calculated frequencies are given for the $TG_2T\bar{G}_2$ model and the $T'G'_2\bar{T}'\bar{G}'_2$ model, respectively. The force constants used in the calculation are shown in Table III, ($TG_2T\bar{G}_2$ and $T'G'_2\bar{T}'\bar{G}'_2$, respectively). [b] Assignment (PED %) are given for the $T'G'_2\bar{T}'\bar{G}'_2$ model; ν, stretching; δ, bending; τ, torsion.

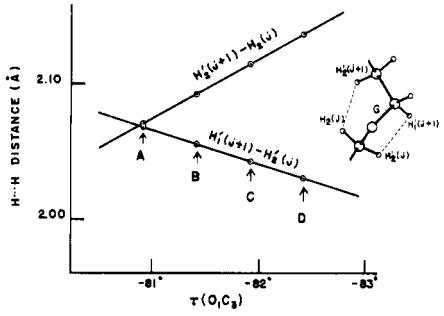

Figure 5. H···H distances with the change of the internal rotation angles.

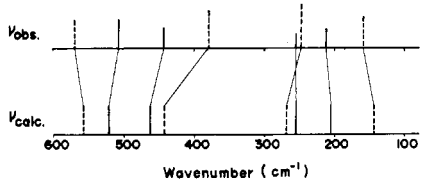

Figure 6. Comparison between the observed (upper) and calculated (lower) normal frequencies of the PEO molecule in the complex of type II.

denote $\tau(O_1C_3)$ and $\tau(C_2O_1)$, respectively, and the values in parentheses give $\tau(C_1C_2)$. The line in the figure indicates such relation between the three internal rotation angles that may satisfy the molecular symmetry and fiber period. Then, the H···H distances were estimated for the points from A to D on the line. In Figure 5 are plotted the distances of the two pairs of the near-hydrogen atoms with the change of the internal rotation angles under conditions a and b. A most plausible model corresponds to point A, where the nearest distance between the hydrogen atoms is equal to 2.07 Å.

$$-CH_2-(-O-CH_2-CH_2-O-CH_2-CH_2-)_n$$
$$\begin{array}{cccccc} T' & G' & G' & \bar{T}' & \bar{G}' & \bar{G}' \\ 167° & 81° & 73° & -167°-81° & & -73° \end{array}$$

Here T′ and G′ denote the internal rotation angles deviating from the exact *trans* (180°) and *gauche* (60°) angles, respectively. The distance between the hydrogen atoms (2.07 Å) may be reasonable in comparison with the van der Waals radius of the hydrogen atom (1.1–1.2 Å.)

Thus the most reasonable model was obtained in terms of infrared absorption, factor group analysis, normal coordinate treatments, and finally the consideration of the van der Waals contacts between the nonbonded hydrogen atoms.

The skeletal normal vibrations were calculated again for the $T'G'_2\bar{T}'\bar{G}'_2$ model with adjusting the force constants so as to fit the calculated frequencies with the observed data. The most plausible set of force constants thus obtained are given in column 3 of Table III, and the calculated frequencies and the potential energy distribution are shown as $T'G'_2\bar{T}'\bar{G}'_2$ in Table IV. In Figure 6 the observed frequencies (upper part) and the calculated frequencies (lower part) are shown schematically in the far-infrared region from 600 to 80 cm^{-1}. The details of the normal coordinate treatment will be published elsewhere.

III. Packing of the PEO Molecule in the Lattice. It

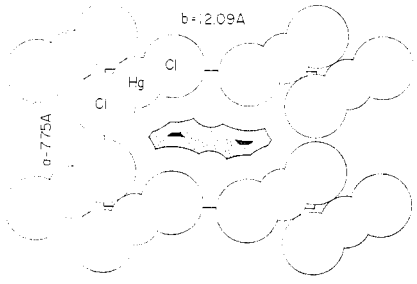

Figure 7. Allowed space for PEO molecules as (x, y, 0) section. The hatched region is available to both the carbon and oxygen atoms, but the dotted region to the oxygen atoms only.

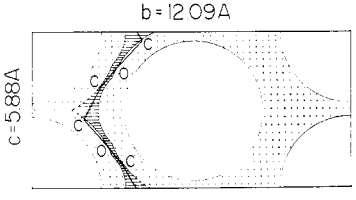

Figure 8. Allowed space for PEO molecules at the (0.48, y, z) section. The hatched and dotted region indicates the same meaning as Figure 7.

is well-known that the interatomic distances between nonbonded atoms or groups cannot be much shorter than their van der Waals distances in the molecular crystal. In the complex type I, the molecular conformation of PEO could be determined by examining the space not occupied by mercuric chloride molecules in the crystal lattice. Here also the space occupied by the $T'G'_2\bar{T}'\bar{G}'_2$ model of PEO in the lattice was examined by the spherical models of the Hg and Cl atoms with their van der Waals radii (Hg, 1.5 Å;[9] Cl, 1.8 Å[5]), coated with the thickness of the van der Waals radii of the CH_2 groups and O atoms (CH_2, 2.0 Å[5] O, 1.4 Å[5]). In Figures 7 and 8 are illustrated the features, for example, at the (x, y, 0) and (0.48, y, z) sections, respectively. In both figures the hatched region can be occupied by both the C and O atoms, but the dotted region can be occupied by the O atoms only. From the feature at the (x, y, 0) section, it was found that the PEO molecules can exist in the neighborhood of $x = 1/2$ and $y = 1/4$ or $3/4$. Then the coordinate of the PEO molecules was determined so as to satisfy the van der Waals contacts in the lattice, as shown in Table V. Here it was taken into account that the glide plane of the PEO molecule may coincide with the c-glide plane ($y = 1/4$ and $3/4$) in the crystal and then an oxygen atom of PEO may be located so as to coordinate to the Hg atoms with the equivalent distance (2.80 Å). The position of the $T'G'_2\bar{T}'\bar{G}'_2$ model of PEO is superimposed, for example, in the (0.48, y, z) section, where the C and O atoms exist not exactly on the plane of the section but on the positions slightly above or below the plane.

IV. Crystal Structure. In order to confirm whether the above-mentioned considerations are correct, the two-dimensional Fourier synthesis $\rho(x, y)$ was examined. The result is shown in Figure 9, where the peaks de-

(9) A. I. Kitajgorodskii, "Cemical Organic Crystallography," Consultants Bureau, New York, N. Y., 1959.

TABLE V

ATOMIC PARAMETERS AND TEMPERATURE FACTORS

Atom	x	y	z	B, Å^2
Hg	0.095	0.151	0.0	5.0
Cl_1	0.253	−0.003	0.0	7.0
Cl_2	0.028	0.680	0.0	5.0
O_1	0.358	0.264	0.774	6.0
O_2	0.358	0.236	0.274	6.0
C_1	0.497	0.221	0.642	6.0
C_2	0.424	0.158	0.435	6.0
C_3	0.497	0.279	0.142	6.0
C_4	0.424	0.342	0.935	6.0

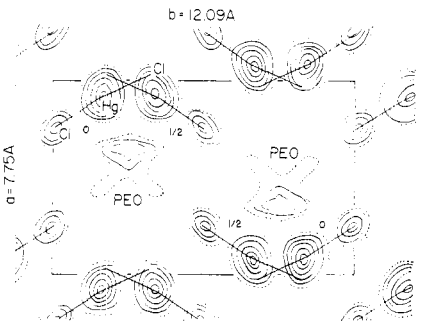

Figure 9. Fourier projection $\rho(x, y)$. The broken curves indicate the contour for 5 electrons/Å^2. The interval of the contours is 20 electrons/Å^2 for Hg, 5 electrons/Å^2 for Cl and PEO.

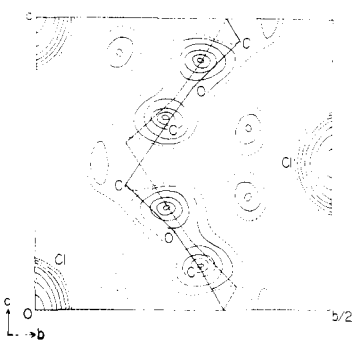

Figure 10. Bounded Fourier projection on the *bc* plane in the range from $x = {}^1/_4$ to ${}^3/_4$. The broken curves indicate the contour for 8 electrons/Å^2. The interval of the contours is 2 electrons/Å^2 for Cl, and 1 electron/Å^2 for PEO.

noted as PEO may be due to the electron density of the PEO molecules projected along the molecular axis. In order to examine the feature of the electron density distribution along the molecular axis, the bounded Fourier projection on the *bc* plane in the range from $x = {}^1/_4$ to ${}^3/_4$ was synthesized as shown in Figure 10. The electron density distribution due to PEO gives good correspondence to the T′G′$_2$T̄′Ḡ′$_2$ model of PEO superimposed as the solid and broken lines. Here these lines relate to each other by the mirror plane ($z = {}^1/_2$). In Figures 9 and 10, the peaks due to the PEO molecule appear almost exactly in the position presumed from the consideration of the van der Waals contacts.

The crystal structure projected to the *ab* and *bc* planes is shown in Figure 11. In Table V are given the atomic coordinates and isotropic temperature factors. The present coordinates of the Hg and Cl atoms were

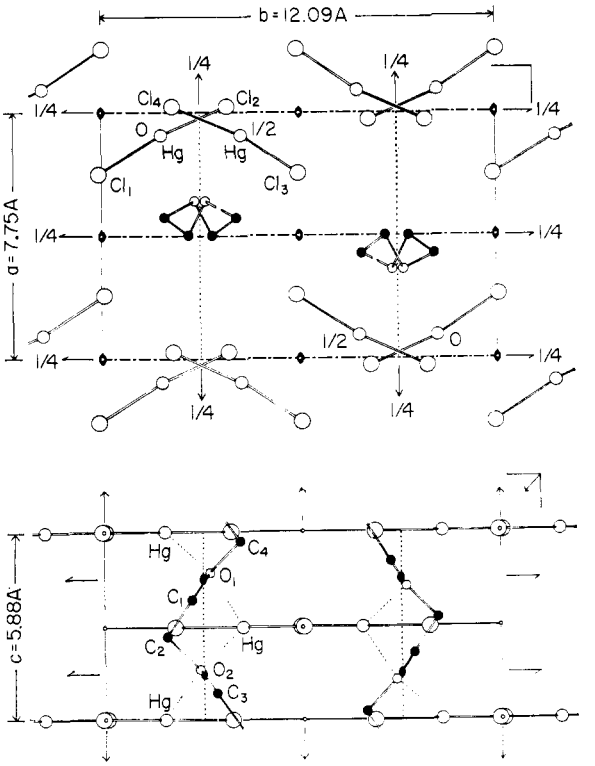

Figure 11. Crystal structure projected on the *ab* plane (upper) and on the *bc* plane (lower).

corrected by the backshift method from the Fourier map. Furthermore, in Table VI are listed the observed and calculated structure factors, especially for the following two cases: (a) $HgCl_2$ molecules only in the lattice, and (b) PEO molecules of the T′G′$_2$T̄′Ḡ′$_2$ conformation in addition to the $HgCl_2$ molecules. Here the effect of the anomalous scattering of the Hg atoms was taken into account, as in the complex of type I. The agreement between the calculated and the observed structure factors was much improved in the latter case, and the discrepancy factor R ($= \sum ||F_o| - |F_c|| / \sum |F_o|$) became 13% from 15%, when the PEO molecules of the T′G′$_2$T̄′Ḡ′$_2$ conformation were taken into account. Thus we could sufficiently confirm the conformation of the PEO molecule and its positions in the crystal lattice.

Discussion

Although the analysis of the crystal structure was performed on the basis of the space group Pncm-D_{2h}^7 in this study, the space group Pnc2-C_{2v}^6 is also possible for the systematic absences of the reflections. The difference between these space groups is due to only the packing of the PEO molecules, while the ways of the packing of the $HgCl_2$ molecules in the lattice are same between the two space groups. A similar problem as to the ways of the packing of the PEO molecules arose in the case of type I as well. In the case of the space group Pncm-D_{2h}^7, a statistically disordered structure with respect to the packing of the PEO molecules is required. Since the PEO molecular chain has no mirror symmetry perpendicular to the fiber axis, it must take statistically with 50% probabilities the two positions symmetrical with respect to the mir-

TABLE VI

STRUCTURE FACTORS[a]

		$\lvert F_c \rvert$				$\lvert F_c \rvert$	
hkl	F_o	$HgCl_2$	PEO–$HgCl_2$	*hkl*	F_o	$HgCl_2$	PEO–$HgCl_2$
1 0 0	229	301	246	0 3 3	119	94	97
1 1 0	132	117	157	2 1 3		3	5
0 2 0	133	69	123	3 3 2	51	47	49
0 1 1	175	193	180	3 5 0	144	135	139
1 2 0	70	109	72	4 2 1	118	111	114
1 1 1	112	102	112	4 3 0	30	34	29
2 0 0	123	93	101	1 3 3	92	90	91
1 2 1	120	137	127	2 6 1	82	70	71
2 1 0	124	171	132	1 7 0	20	20	15
1 3 0	34	40	20	2 5 2	129	126	114
0 3 1	124	132	116	3 5 1	20	18	16
2 2 0	119	105	107	2 2 3	150	132	133
2 1 1	54	15	18	4 3 1	135	136	131
1 3 1	156	138	154	0 6 2	173	158	168
0 4 0	147	146	127	0 7 1	218	152	151
0 0 2	327	317	302	1 6 2	119	113	105
2 2 1	228	207	219	4 4 0	108	94	95
2 3 0	85	64	82	3 4 2	14	20	13
1 4 0	171	154	165	1 7 1	107	106	105
1 0 2	237	224	227	4 0 2	60	59	61
1 1 2	112	90	79	1 4 3	53	51	52
0 2 2	52	56	40	2 3 3	47	45	46
3 0 0		6	9	4 1 2	54	60	53
3 1 0	177	145	161	2 7 0	50	33	37
1 2 2	98	81	89	3 6 0	10	4	8
1 4 1	82	80	73	4 4 1	64	68	71
2 3 1	75	73	68	4 2 2	31	36	34
2 4 0	140	100	101	5 0 0	93	111	113
3 2 0	20	6	15	3 1 3	20	23	24
2 1 2	149	134	142	2 6 2	51	39	37
1 5 0	105	108	100	3 6 1	83	60	60
1 3 2	53	31	45	5 1 0		2	3
0 5 1		8	1	0 5 3	10	3	8
3 2 1	184	187	178	2 4 3	69	76	75
2 4 1	129	117	125	2 7 1	26	27	29
2 2 2	84	75	79	3 2 3	111	122	121
3 3 0	58	59	56	3 5 2	105	111	115
1 5 1	41	25	18	4 5 0	116	76	70
0 4 2	128	119	139	0 8 0	58	29	35
3 3 1	56	65	65	5 2 0	52	27	32
2 5 0	135	155	160	4 3 2	54	28	32
1 4 2	93	121	109	1 5 3	32	15	19
2 3 2	32	50	38	5 1 1	75	75	77
0 6 0	215	198	189	1 8 0		6	5
3 4 0	30	25	30	0 0 4	100	156	157
0 1 3	110	111	110	3 3 3	50	42	43
2 5 1	50	49	51	1 0 4	133	115	114
3 0 2	14	7	17	1 7 2	25	16	22
4 0 0	74	69	78	4 5 1		1	0
1 6 0	138	140	142	5 2 1	24	30	29
3 1 2	116	117	121	1 1 4	43	48	53
4 1 0	94	74	76	3 7 0	19	30	31
1 1 3	61	65	66	1 8 1	36	59	58
1 6 1	53	50	50	5 3 0		9	11
3 2 2		4	5	0 2 4	22	34	36
2 4 2	78	77	73	2 5 3	23	29	26
3 4 1	105	106	100	4 4 2	68	76	80
4 2 0	50	46	49	1 2 4	32	42	42
1 2 3	91	85	85	3 6 2		4	4
4 1 1	51	50	48	5 3 1	107	112	114
1 5 2	104	86	98	2 8 0	22	21	22
2 6 0	62	46	50				

TABLE VI (*Continued*)

hkl	F_o	$\lvert F_c \rvert$ HgCl₂	$\lvert F_c \rvert$ PEO–HgCl₂	*hkl*	F_o	F_c HgCl₂	F_c PEO–HgCl₂
3 4 3	94	71	71	2 1 4	64	73	69
4 6 0	50	37	40	1 3 4	13	17	14
3 7 1	28	19	21	2 8 1	89	94	96
2 7 2	29	27	22	4 6 1	56	34	34
1 6 3	41	33	31	2 2 4	25	36	31
2 0 4	50	43	38	4 2 3	59	74	75
4 1 3	33	36	35	0 8 2	15	23	19
5 4 0	66	78	71	4 5 2	50	62	65

[a] The F_o values with a brace are the structure factors estimated as proportional to the observed data on the fiber diagram, or to the corresponding $|F_c|$ for PEO–HgCl₂. Since the calculated structure factors, F_c, are complex because they include the effect of the anormalous scattering of the Hg atom, their absolute values are listed.

TABLE VII

THE BOND LENGTH, BOND ANGLE, AND ANTISYMMETRIC STRETCHING VIBRATION (ν_a) OF THE $HgCl_2$ MOLECULE

	Hg–Cl₁, Å	Hg–Cl₂, Å	∠ClHgCl, deg	ν_a, cm⁻¹
$HgCl_2$ crystal	2.23[a]	2.27	180	367[b]
Type I	2.30	2.30	176	353
Type II	2.23	2.25	172	345

[a] Data of H. Bräkken and W. Schloten, *Z. Krist.*, 89, 448 (1934). [b] Data of W. Klemperer and L. Lindeman, *J. Chem. Phys.*, 25, 397 (1956).

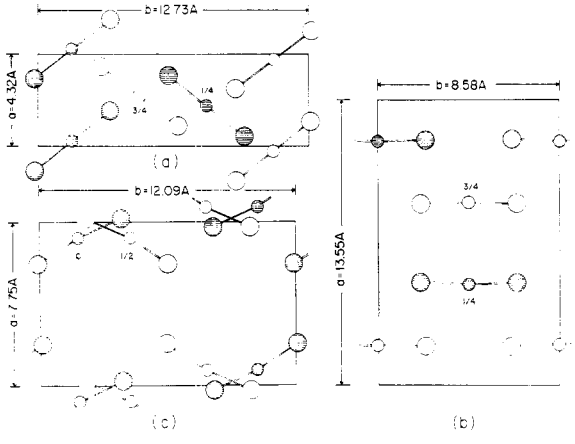

Figure 12. Packing features of $HgCl_2$ molecules in (a) $HgCl_2$ crystal, (b) PEO–$HgCl_2$ complex of type I, and (c) PEO–$HgCl_2$ complex of type II.

ror plane at $z = 0$ and $1/2$. In the case of the space group Pnc2-C_{2v}^6, however, it is not necessary to take account of such a statistically disordered structure, since this space group has not the mirror symmetry at $z = 0$ and $1/2$. In fact, it is difficult to determine from the present X-ray data which of the space group is reasonable.

In both cases of type I and type II, it was found that the $HgCl_2$ molecule is distorted slightly from the linear form as shown in Table VII. Such distortions of the $HgCl_2$ molecules may be caused by the way of coordination to the O atoms of the PEO molecule. The $HgCl_2$ molecules in the complex of type II bend from the linear form in the opposite direction of that in the complex of type I, where the two Cl atoms bonded to a Hg atom are distored so as to apart slightly from the PEO molecule. The packing of the $HgCl_2$ molecules in type II is much closer than that in type I, and the nearest Cl···Cl distance is 3.40 Å ($Cl_2 \cdots Cl_4$ in Figure 11). This value is smaller than the sum of the van der Waals radii of chlorine atoms (3.6 Å). Such steric repulsion may be one of the factors of the distortion in the case of type II.

In Figure 12 is shown the packing features of (a) $HgCl_2$ crystal, (b) PEO–$HgCl_2$ complex of type I, and (c) type II. The crystal structure[10,11] of $HgCl_2$ is orthorhombic with the lattice constants $a = 4.325$ Å, $b = 12.735$ Å, and $c = 5.963$ Å.[12] The unit cell consists of two layers, each containing two $HgCl_2$ molecules. In this case as well as in type II, the two Cl atoms bonded to a Hg atom are not crystallographically equivalent to each other and lie on the mirror plane. There is some interesting resemblance between the ways of packing of the $HgCl_2$ molecules in these two crystals. The length of c axis of the $HgCl_2$ crystal (5.963 Å), for example, is almost equal to the fiber period of type II crystal (5.88 Å), and moreover the lengths of the b axis of these two crystals are almost the same with each other. These facts suggest that the lattice formation of type II may be affected predominantly by the arrangement of the $HgCl_2$ molecules. The elongation of the a axis may be caused by the entry of the PEO molecules as shown in Figure 11.

It is known that the internal rotation angles about the C–O bonds in the PEO molecule easily take the *trans* form rather than the *gauche* form because of the van der Waals contacts between the nonbonded hydrogen atoms, and actually in the pure polymer as well as the complex of type I, all the C–O bonds take the *trans*

(10) H. Bräkken and L. Harang, *Z. Krist.*, **68**, 123 (1928).
(11) See Table VII, footnote *a*.
(12) The *a* and *c* axes are exchanged from the original paper for the convenience of comparison.

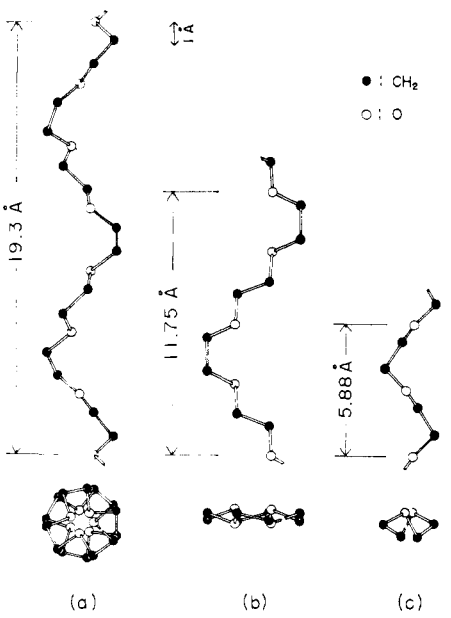

Figure 13. Molecular conformations of PEO in various states: (a) ordinary PEO, $(T'_2G')_7$; (b) complex of type I, $T_3GT_3\bar{G}$; and (c) complex of type II, $T'G'_2\bar{T}'\bar{G}'_2$.

form. On the contrary, in the complex of type II one of the two C–O bonds does not take *trans* form, but takes the angle near to the *gauche* or minus-*gauche* form (81 or −81°). In Figure 13 is shown the molecular model of PEO in type II, together with the ordinary PEO molecule and that in type I. The fact that the C–O bonds in type II take such internal rotation angles, though considerably distorted from the exact *gauche* form, seems to contradict with the above-mentioned sense. The $HgCl_2$ molecules of type II, as already discussed, is similar to that of the $HgCl_2$ crystal in point of the lattice dimension and of their arrangements. Taking account of this fact, it may be considered that a primary factor in taking such a conformation unstable in the ordinary PEO molecules is due to the interaction with the $HgCl_2$ molecules. Furthermore, one of the factors that the C–O bonds take the angle distorted considerably from the exact *gauche* form may be due to the repulsion between the nonbonded hydrogen atoms besides to the interaction with the $HgCl_2$ molecules.

In Table VII the Hg–Cl bond lengths and frequencies of the antisymmetric stretching vibration of the $HgCl_2$ molecules are compared in the different states. Although the bond length 2.30 Å in type I is somewhat longer than that in $HgCl_2$ crystal (2.23 and 2.27 Å),[11] it is found that the bond lengths in type II ($Hg–Cl_1$ = 2.23 Å and $Hg–Cl_2$ = 2.25 Å) are almost equal to that in the $HgCl_2$ crystal. In the infrared spectra, however, we observed the frequency shifts of the antisymmetric stretching vibration from 367 cm^{-1} in the $HgCl_2$ crystal[13] to the lower frequency side 353 cm^{-1} in type I, furthermore to 345 cm^{-1} in type II. We could not find a simple correlation between the Hg–Cl bond length and frequency of the $HgCl_2$ antisymmetric stretching.

It is also interesting that the PEO molecules make the two types of complexes coordinating to $HgCl_2$ molecules. In the present study, it is considered that the each oxygen atom of the PEO molecule coordinates to two Hg atoms with an equivalent distance and angle HgOHg = 85.° It remains as a problem for further study what kind of intermolecular force may act in those complexes.

Acknowledgment. We wish to thank Drs. Y. Chatani and M. Kobayashi of this laboratory for their kind advice and fruitful discussion.

(13) See Table VII, footnote *b*.